NANO LETTERS

Letter

pubs.acs.org/NanoLett

A Nanostructured Conductive Hydrogels-Based Biosensor Platform for Human Metabolite Detection

Lanlan Li,[†] Yaqun Wang,[‡] Lijia Pan,*[,†] Ye Shi,[‡] Wen Cheng,[†] Yi Shi,*[,†] and Guihua Yu*[,‡]

[†]Jiangsu Provincial Key Laboratory of Photonic and Electronic Materials, School of Electronic Science and Engineering, Collaborative Innovation Center of Advanced Microstructures, Nanjing University, Nanjing 210093, China

[‡]Materials Science and Engineering Program and Department of Mechanical Engineering, The University of Texas at Austin, Austin, Texas 78712, United States

Supporting Information

ABSTRACT: The development of a scalable, low-cost, and versatile biosensor platform for the sensitive and rapid detection of human metabolites is of great interest for healthcare, pharmaceuticals, and medical science. On the basis of hierarchically nanostructured conducting polymer hydrogels, we designed a flexible biosensor platform that can detect various human metabolites, such as uric acid, cholesterol, and triglycerides. Owing to the unique features of conducting polymer hydrogels, such as high permeability to biosubstrates and rapid electron transfer, our biosensors demonstrate excellent sensing performance with a wide linear range (uric acid, 0.07−1 mM; cholesterol, 0.3−9 mM, and triglycerides, 0.2−5 mM), high sensitivity, low sensing limit, and rapid response time (~3 s). Given the facile and scalable processability of hydrogels, the proposed conductive hydrogels-based biosensor platform shows great promise as a low-cost sensor kit for healthcare monitoring, clinical diagnostics, and biomedical devices.

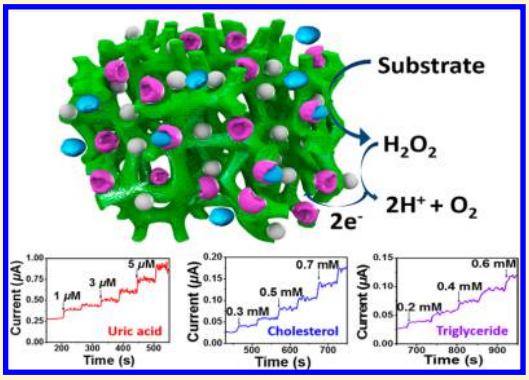

KEYWORDS: *Conductive polymers, hydrogel, biosensor, human metabolite, uric acid, cholesterol, triglyceride*

The estimation of metabolites, such as glucose, urea, cholesterol, and triglycerides, in whole blood is of central importance in clinical diagnostics.[1−3] An imbalance of blood metabolites is considered to be one of the most severe threats to human health and is related to high risks of several serious illnesses. For example, high levels of cholesterol and triglycerides in the blood are closely associated with cardiovascular diseases, such as atherosclerosis, hypertension, and cardiopathy;[4−12] high uric acid levels in the human body cause gout.[13−16] Such metabolite complications can be greatly reduced through stringent personal control of blood metabolite concentration. Therefore, extensive research has been focused on the development and exploitation of analytical devices for the detection, quantification, and monitoring of blood metabolite levels. Amperometric enzyme electrodes for glucose,[17,18] uric acid,[19,20] cholesterol,[21,22] and triglycerides[23,24] have been developed with various electrode materials, such as eggshell membranes,[14] chitosan,[6] multiwalled carbon nanotubes,[25,26] and graphene, among others.[27] Among the various materials developed thus far, conducting polymer hydrogels (CPHs) hold particular promise as low-cost and high-performance biosensor electrode materials.[17,18] CPHs are hydrophilic, conductive, polymeric materials with physically or chemically cross-linked networks that can absorb large amounts of water without being dissolved. By synergizing the advantages of both hydrogels and organic conductors,[28] CPHs exhibit favorable features as biosensor materials, such as high permeability to biomolecules, biocompatibility, and rapid electron transfer.

Despite the rapid development of electrode materials, it remains challenging to develop biosensing platforms that can detect all metabolites simultaneously with high sensitivity, a wide linear range and rapid response time, while being compatible with simple patterning technology, which is critical for the low-cost fabrication and integration of sensor kits and multiplex sensors for healthcare monitoring, clinical diagnostics, and biomedical devices.[29,30]

To solve these crucial problems, we developed a biosensor platform based on a Pt nanoparticle (PtNP)-modified CPH electrode. Our CPH-based biosensor platform was produced in an all-solution process and presents excellent sensing performance to uric acid, cholesterol, and triglyceride metabolites with wide linear ranges (uric acid, 0.07−1 mM; cholesterol, 0.3−9 mM; and triglycerides, 0.2−5 mM), high sensitivities, low sensing limits and rapid response times (~3 s). The simple fabrication and high sensitivity to multiple metabolites demonstrates the promising application of our CPH-based biosensor platform for producing low cost biosensor kits on a large scale.

Received: November 3, 2014
Revised: December 20, 2014
Published: January 8, 2015

DOI: 10.1021/nl504217p
Nano Lett. 2015, 15, 1146−1151

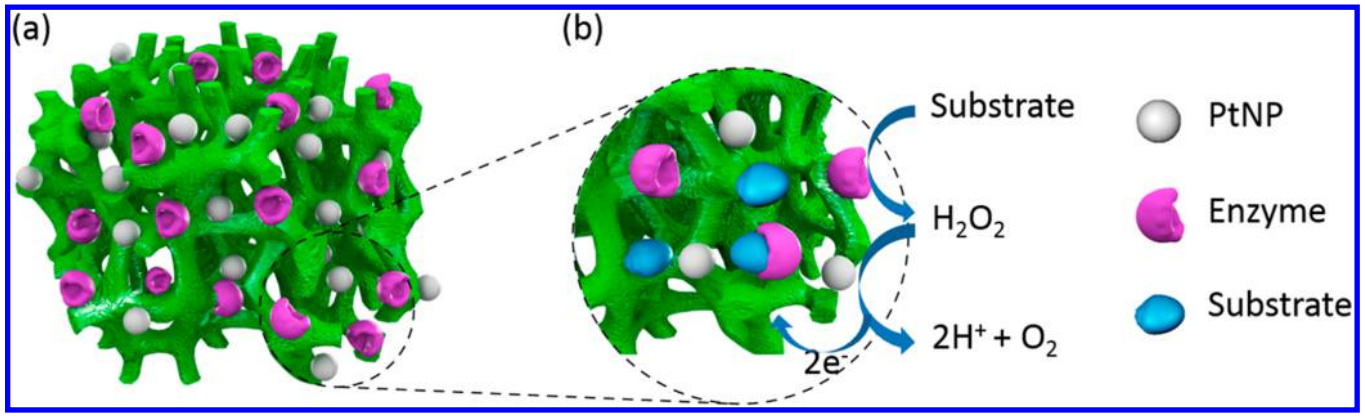

Figure 1. Schematic illustration of the general sensing mechanism of our CPH-based electrode platform. (a) PtNPs and enzymes were loaded onto hierarchically three-dimensional (3D)-porous PAni hydrogel matrices to form PAni hydrogel/PtNPs hybrid electrodes. (b) The PtNP-catalyzed sensing process of the biosensor based on PAni/PtNPs/enzyme hybrid films.

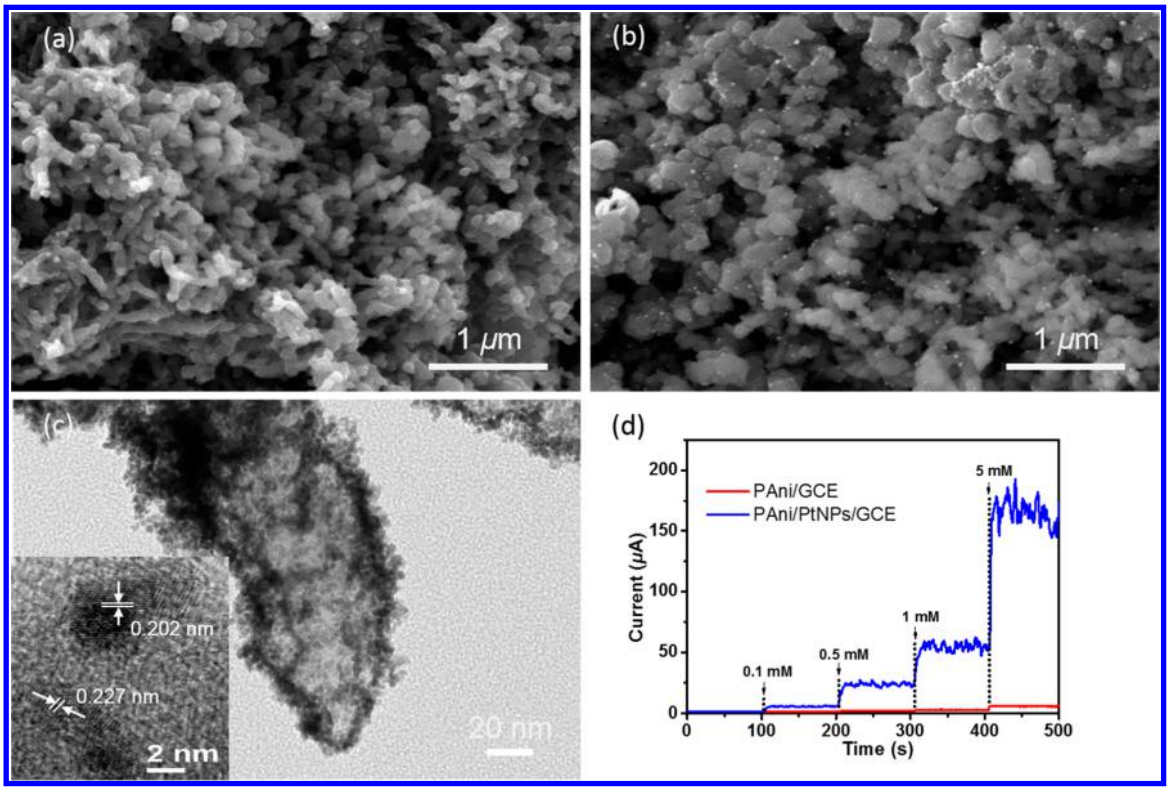

Figure 2. Morphology of a PAni hydrogel and PAni/PtNPs hybrid film. (a) SEM image of bare PAni hydrogel. (b) SEM image indicating that homogeneous PtNPs were loaded onto the hydrogel matrix. (c) TEM image of a PAni hydrogel with embedded PtNPs. Inset: HR-TEM image of PtNPs in a PAni hydrogel. (d) Comparison of the sensing performance of a bare PAni hydrogel (red curve) and PAni hydrogel/PtNPs (blue curve) electrodes with the instant amperometric response corresponding to the successive addition of hydrogen peroxide.

The sensing mechanism of the proposed biosensor platform based on a CPH/PtNPs/enzyme hybrid electrode is illustrated in Figure 1. Polyaniline (PAni) hydrogels provide hierarchically porous, nanostructured matrices, and particularly, solvated surfaces resulted from the hydrophilic nature of the hydrogels. These features are favorable for enhanced molecule permeability. Our PAni hydrogel framework exhibits good electronic conductivity, and their conducting nature from conjugated polymer improves the electric interface, enhancing rapid electron transfer between the enzyme and electrode. PtNPs were homogeneously dispersed in the hydrogel matrix to catalyze the electrochemical oxidization of the hydrogen peroxide molecules generated in the enzymatic reaction between the substrates and enzymes and to enhance the current collection in electrochemical processes. This working mechanism is general and efficient. Thus, our hydrogel-based hybrid electrodes can be used as a highly sensitive platform to detect different metabolites by immobilizing different enzymes that are selectively catalytic to a specific metabolite.

A PAni/PtNP-modified glassy carbon electrode (GCE) was used as the working electrode for the biosensors. Drops of two solutions were mixed and coated onto the GCE, one containing aniline monomer and phytic acid and the other containing the polymerization initiator. Phytic acid acts as both cross-linker and doping agent. The coated solution was gelated to form a hydrogel thin film within 3 min. After purification and drying,

DOI: 10.1021/nl504217p
Nano Lett. 2015, 15, 1146−1151

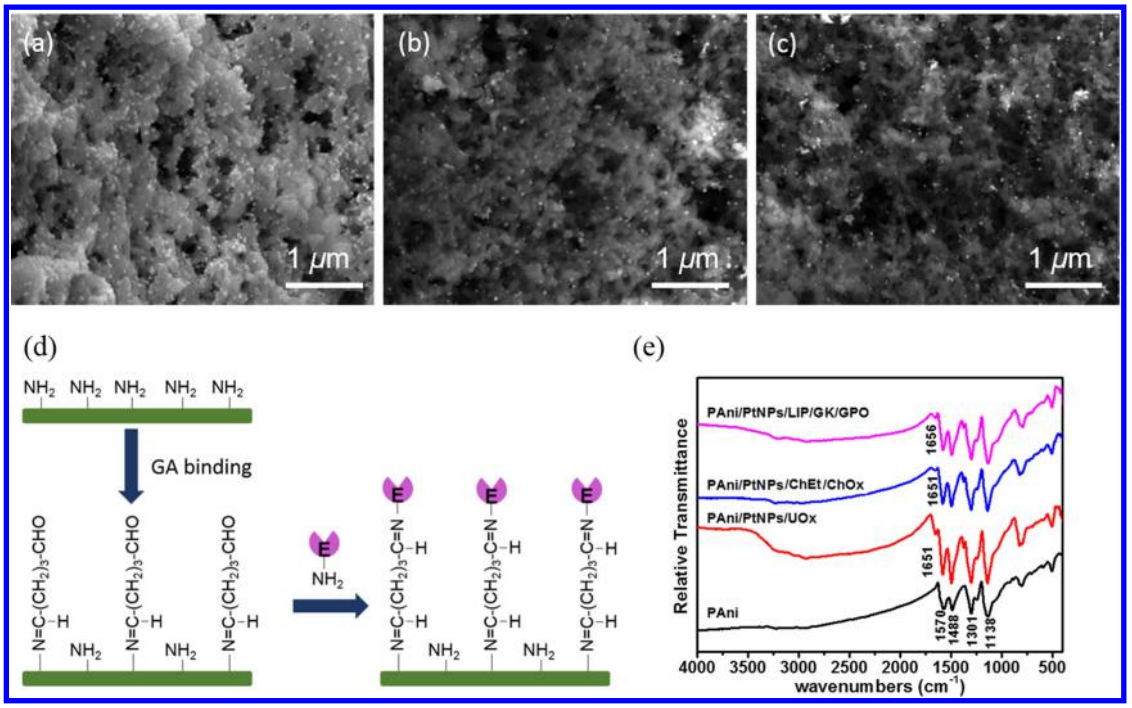

Figure 3. Morphologies of PAni/PtNPs electrodes immobilized with different enzymes. (a–c) SEM images of PAni/PtNPs/UOx, PAni/PtNPs/ChEt/ChOx and PAni/PtNPs/LIP/GK/GPO biosensors. (d) Schematic diagram of the covalent immobilization of enzymes onto a PAni hydrogel with bifunctional compound GA. (e) FT-IR spectra of bare PAni and the following materials: PAni, PAni/UOx/GA, PAni/ChEt/ChOx/GA, and PAni/LIP/GK/GPO/GA.

the thin film was put into contact with a solution of chloroplatinic acid and formic acid to generate PtNPs on the hydrogel matrix.

The morphologies and structures of the PAni hydrogel/PtNPs were characterized using scanning electron microscopy (SEM) and transmission electron microscopy (TEM), as shown in Figure 2. Figure 2a depicts the typical morphology of a PAni hydrogel with a 3D-porous morphology, which consists of interconnected nanofibers with uniform diameters ranging from 60 to 100 nm. As shown in the SEM image in Figure 2b and the TEM image in Figure 2c, homogeneous PtNPs with diameters of approximately 3 nm were embedded in the PAni hydrogel matrix with high density. A high-resolution (HR)-TEM image of the PtNPs is shown in the inset of Figure 2c. The lattice spacing of 0.202 and 0.227 nm correspond to the Pt(200) and Pt(111) planes, respectively.[31] Notably, the monodisperse PtNPs played an important role in enhancing the performance of the biosensor because PtNPs catalyzed the electrochemical oxidization of the hydrogen peroxide molecules generated during the enzymatic reaction (Figure 1b). This catalytic reaction significantly increased the current collected on the electrode, as shown in Figure 2d, which compared the sensing performance for hydrogen peroxide of PAni/GCE and PAni/PtNPs/GCE at a potential of 0.4 V. For the same concentration of hydrogen peroxide, the current of the GCE coated with PAni/PtNPs was greatly increased compared with that of the GCE coated with only a PAni hydrogel, confirming the efficient catalytic effect for the electro-oxidation of hydrogen peroxide by the high-density and monodisperse PtNPs in the PAni hydrogel matrix. The sensing performances of enzyme biosensors can be greatly improved by an enhanced response to hydrogen peroxide molecules.

The immobilization of enzymes is one of the key factors affecting the performance of biosensors. We used a bifunctional compound, glutaraldehyde (GA), to cross-link the enzymes in the PAni hydrogel matrix (Figure 3). The SEM images of the PAni hydrogel/PtNPs immobilized with enzymes are shown in Figure 3a–c, corresponding to the immobilization of uricase (UOx), cholesterol esterase/cholesterol oxidase (ChEt/ChOx), and lipase/glycerol kinase/glycerol-3-phosphate oxidase (LIP/GK/GPO), respectively. The enzymes were homogeneously deposited on the PAni 3D nanostructures at high density, possibly due to the good wetting of the enzyme solution on the hydrophilic hydrogel matrix. The evenly thin coating of enzymes on PAni matrix is significant for sensing performance due to the decreased path length for molecules and electrons. The enzyme immobilization mechanism is schematically illustrated in Figure 3d; PAni hydrogels possess an abundance of amino groups at the surface of the PAni fibers, which were bonded to the amino groups on the enzymes, forming covalent C═N bonds by reacting with the two aldehyde groups on the GA. Thus, different UOx, ChEt/ChOx, and LIP/GK/GPO enzymes can be efficiently immobilized on our hydrogel matrices. The chemical immobilization of enzymes on the PAni/PtNPs films was confirmed using Fourier transform infrared (FT-IR) spectroscopy. The PAni spectrum of the hydrogel was in accordance with that of emeraldine PAni. Compared with the spectrum of bare PAni, the additional peaks at 1651 cm^{-1} for PAni/UOx/GA and PAni/LIP/GK/GPO/GA and at 1656 cm^{-1} for PAni/ChEt/ChOx/GA were assigned to the stretching vibration of the covalent C═N bonds,[15] indicative of the covalent cross-linking between the enzymes and the hydrogel matrix.

The PAni/PtNPs/enzyme hybrid electrodes were studied using cyclic voltammetry (CV) and chronoamperometry in a three-electrode configuration in phosphate buffer solution (PBS), as shown in Figure 4. The comparison of bare GCE, PAni/GCE, PAni/PtNPs/GCE, and PAni/PtNPs/GCE/en-

DOI: 10.1021/nl504217p
Nano Lett. 2015, 15, 1146–1151

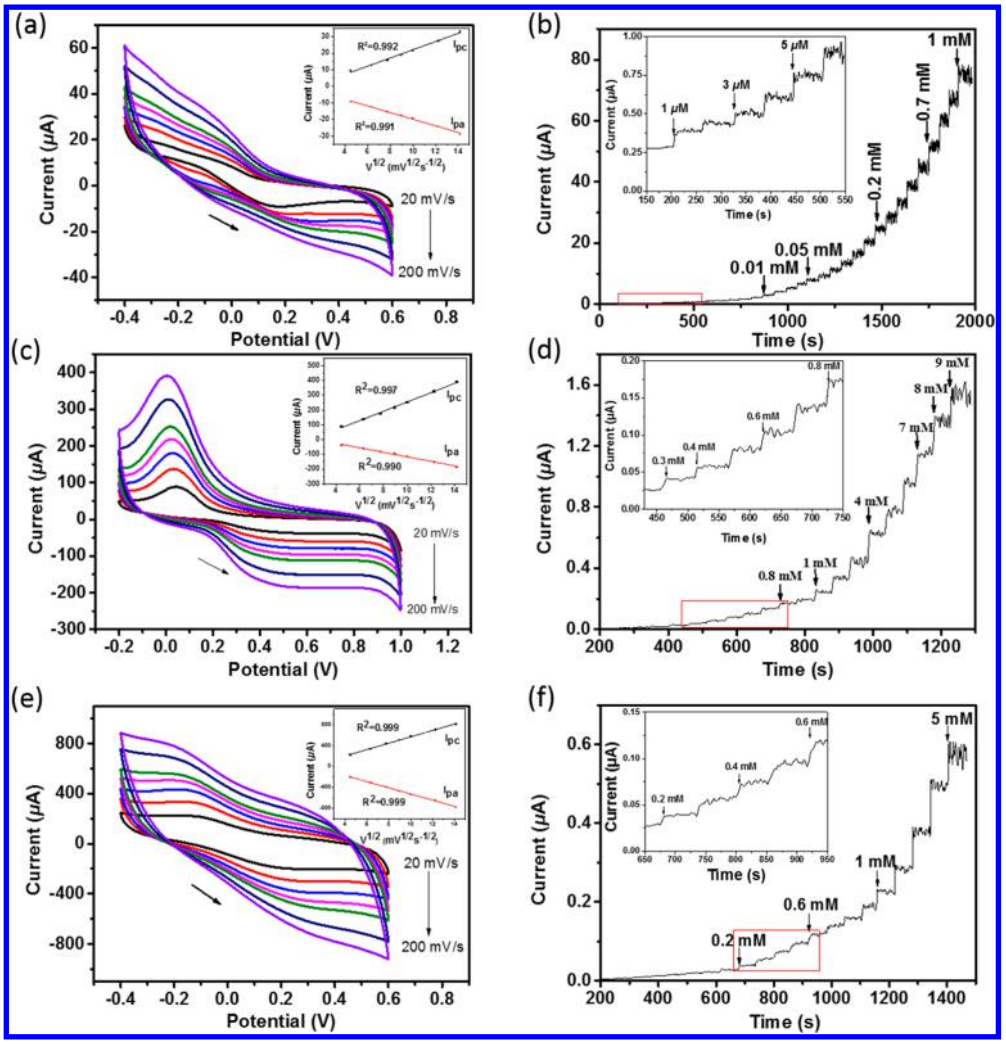

Figure 4. Electrochemical CV measurements (a,c,e) in PBS at different scan rates (20, 40, 60, 80, 100, 150, and 200 mV/s) and instant current−time response curves of metabolites being successively added in PBS solutions (b,d,f). (a,b) PAni/PtNPs/UOx, (c,d) PAni/PtNPs/ChEt/ChOx, and (e,f) PAni/PtNPs/LIP/GK/GPO bioelectrodes. Insets in a,c,e represent the anodic and cathodic peak current variation as a function of square root of scan rate. Insets in b,d,f represent magnified views of the curve region marked within the red square.

Table 1. Comparison of the State-of-Art Analytical Performance of Different Biosensors

substrate	immobilization matrix	linearity (mM)	detect limit (mM)	response time (s)	sensitivity ($\mu A \cdot mM^{-1} \cdot cm^{-2}$)	Km (mM)	ref
uric acid	Ir−C/Au	0.1−0.8	0.01	24.7−40.8	155.5	NR	32
	Chi−CNTsNF/AgNPs/Au	0.001−0.4	0.001	NR	218.3 ± 7.0	0.21	13
	MPx-11/Au	0.005−0.15	0.002	80−100	3.4 ± 0.08	0.29	20
	Trp-GR/GCE	0.01−1	0.00124	NR	NR	NR	34
	PAni-PB/Pt	0.01−0.16	0.0026	NR	160	0.034	35
	PAni-PtNPs/GCE	0.07−1	0.001	3	322.8	0.347	this work
cholesterol	PAni-Au-CH/ITO	1.3−12.9	0.98	20	33.08	0.28	8
	nNiO-MWCNT/ITO	0.25−12.93	0.03	2	2200	0.22	26
	PAni/ITO	0.8−7.7	NR	40	5×10^{-5}	NR	36
	PAni/ITO	0.8−7.7	0.38	240	2.8	1.15	37
	PPy-Nf/PB/SAM/Pt	0.05−0.3	0.012	NR	8.6	0.09	38
	PAni-PtNPs/GCE	0.3−9	0.3	3	0.88	1.17	this work
triglyceride	PAni-SWCNT/ITO	1.65−13.2	NR	12	12.97	1.14	24
	NPG/GCE	1.65−8.27	0.09	NR	9.09	0.35	23
	NiONPs-CHIT/ZnO-ZnHCF/Au	0.56−7.9	0.11	4	19.29	NR	39
	CA/Pt	0.2−3.5	0.2	40	NR	NR	40
	AuNPs/PEDOT−PSS/SPCE	0.1−6	0.09	30	2.66	NR	5
	PAni-PtNPs/GCE	0.2−5.0	0.2	3	0.57	2.51	this work

DOI: 10.1021/nl504217p
Nano Lett. 2015, 15, 1146−1151

zyme electrodes is presented in Supporting Information S2. The CV responses for the PAni/PtNPs/UOx (Figure 4a), PAni/PtNPs/ChEt/ChOx (Figure 4c), and PAni/PtNPs/LIP/GK/GPO (Figure 4e) bioelectrodes were recorded at different scan rates ranging from 20 to 200 mV/s. As higher scan rates were applied, the anodic peak potentials shifted more to positive potential, and the cathodic peak potentials shifted more toward negative potential. Moreover, nearly perfect linear relationships between the peak currents (I_{pa} and I_{pc}) and the square root of the scan rates ($v^{1/2}$) with a square of regression coefficient (R^2) of 0.99 for the three biosensors (insets of Figure 4a,c,e) were observed, indicating that the electron transfer processes of these electrodes were diffusion-controlled processes.

Figure 4b,d,f demonstrates the amperometric response of the PAni/PtNPs/UOx, PAni/PtNPs/ChEt/ChOx, and PAni/PtNPs/LIP/GK/GPO hybrid electrodes. The electrochemical measurements were performed by separate, successive addition of uric acid, cholesterol oleate, and triolein into PBS. As shown in the current−time curves, the currents immediately increased upon addition of the substrates, promptly reaching a steady state with an average response time of approximately 3 s, which is much faster than previously reported sensors using different electrode materials, such as single-walled carbon nanotubes (SWCNTs), ZnO, and chitosan (see Table 1 for detailed comparison). The steady currents of the biosensors as a function of concentration show linear relationships within a certain concentration range. For the detection of uric acid, our biosensor demonstrates a wide linear range from 0.07 to 1 mM, including the normal level of uric acid in human serum (between 0.13 and 0.46 mM[32]) with a correlation coefficient of 0.994 (see Supporting Information S3 for details) and a lower detection limit of 1 μM (S/N = 3). The sensitivity of the uric acid biosensor was calculated to be 322.8 $\mu A \cdot mM^{-1} \cdot cm^{-2}$, which is significantly higher than the sensitivities of the previously reported biosensors listed in Table 1. Ideally, the total cholesterol concentration in a healthy person's blood should be less than 5.17 mM. The borderline high is defined as 5.17−6.18 mM and the high value is defined as above 6.21 mM.[33] Our cholesterol biosensor presents a linear relationship between the steady current and cholesterol concentration in the range of 0.3 to 9 mM, which is broader than the normal level of cholesterol in human serum and comparable to or broader than previously reported values for the biosensors listed in Table 1. The correlation coefficient was calculated to be 0.997 (Supporting Information, Figure S2b), and the sensitivity was 0.88 $\mu A \cdot mM^{-1} \cdot cm^{-2}$. The inset in Figure 3d demonstrates that the detection limit of our cholesterol biosensor was 0.3 mM.

High concentrations of triglycerides can cause high risk of hyperlipidemia, and triglyceride-detecting biosensors should cover all of the normal ranges in human serum, which are 0.45−1.8 mM for men and 0.4−1.53 mM for women.[24] From the amperometric responses of the triglyceride biosensor to successive additions of triolein, we computed a linear range of 0.2−5 mM, with a correlation coefficient of 0.992 (Supporting Information Figure S2c) and a sensitivity of 0.57 $\mu A \cdot mM^{-1} \cdot cm^{-2}$. The detection limit of the triglyceride-based PAni/PtNPs-modified electrode was calculated to be 0.2 mM. Compared with the different state-of-art biosensors listed in Table 1, the performance of our PAni hydrogel/PtNPs/GCE sensor platform was comparable/superior due to its wide linear range (covering all required detection ranges of uric acid, cholesterol and triglyceride in human serum), fast response times, high sensitivities, and low detection limits.

It is known that enzyme is highly specific for substrate. The specificity of the PAni/PtNPs/enzyme hybrid electrodes is closely related to the property of enzymes immobilized on the PAni hydrogel matrix. In present work, 1 mM urea, 1 mM lactic acid and 5 mM glucose were added into the PBS for the detection of uric acid, cholesterol, and triglyceride. As shown in Supporting Information Figure S2, the easily oxidized species of urea, lactic acid, and glucose with their normal concentration in human blood almost have no effect to the biosensors (see Supporting Information S4 for details). The result confirmed that the PAni/PtNPs/enzyme biosensor platforms have a good anti-interference ability. The invertibility of the response of the PAni/PtNPs/enzyme bioelectrodes was also investigated by successive addition and dilution the concentration of substrates (see Supporting Information S5 for details). The biosensors presented almost the same signals for the same concentrations, indicating that the PAni/PtNPs/enzymes biosensors have good repeatability and reproducibility as well as showing the potential to monitor substrates concentration continuously.

In summary, we have demonstrated a general yet powerful biosensor platform based on conducting polymer hydrogel electrodes. The biosensor platform exhibited an unprecedented performance for detecting a series of metabolites, such as uric acid, cholesterol, and triglycerides. These biosensors achieved excellent sensing capabilities to these metabolites with wide linear ranges that covered the full range of the metabolites in human serum, rapid response times (approximately 3 s), high sensitivities, and low detection limits. All of these features suggest that our conductive polymer hydrogels will lead to an exciting future and intriguing discoveries of hydrogel-based electronics for low-cost and large-scale biosensor and biomedical device kits, which will be highly attractive for the development of healthcare monitoring and clinical diagnostics.

■ ASSOCIATED CONTENT

Ⓢ Supporting Information

Experimental details, further measurement of analysis, and other control experiments. This material is available free of charge via the Internet at http://pubs.acs.org.

■ AUTHOR INFORMATION

Corresponding Authors

*E-mail: (L.P.) ljpan@nju.edu.cn.
*E-mail: (Y.S.) yshi@nju.edu.cn.
*E-mail: (G.Y.) ghyu@austin.utexas.edu.

Author Contributions

L.L. and Y.W. contributed equally to this work.

Notes

The authors declare no competing financial interest.

■ ACKNOWLEDGMENTS

G.Y. acknowledges the financial support of faculty start-up grant from the University of Texas at Austin, and the Welch Foundation Grant F-1861. L.P. and Y.S. are grateful for funding support from the Chinese National Key Fundamental Research Project (2013CB932900, 2011CB92210), the National Natural Science Foundation of China (61229401, 61076017, 60990314, and 41401257), Natural Science Fundation of Jiangsu (BK2011011, BK20130055, and BK20141054), and the NCET and the PAPD Programs.

DOI: 10.1021/nl504217p
Nano Lett. 2015, 15, 1146−1151

REFERENCES

(1) Gerard, M.; Chaubey, A.; Malhotra, B. D. *Biosens. Bioelectron.* **2002**, *17*, 345−359.
(2) Dhand, C.; Das, M.; Datta, M.; Malhotra, B. D. *Biosens. Bioelectron.* **2011**, *26*, 2811−2821.
(3) Wang, J. *Chem. Rev.* **2008**, *108*, 814−825.
(4) Pundir, C. S.; Narang, J. *Int. J. Biol. Macromol.* **2013**, *61*, 379−89.
(5) Phongphut, A.; Sriprachuabwong, C.; Wisitsoraat, A.; Tuantranont, A.; Prichanont, S.; Sritongkham, P. *Sensor. Actuators, B* **2013**, *178*, 501−507.
(6) Narang, J.; Chauhan, N.; Rani, P.; Pundir, C. S. *Bioprocess. Biosyst. Eng.* **2013**, *36*, 425−32.
(7) Narang, J.; Pundir, C. S. *Int. J. Biol. Macromol.* **2011**, *49*, 707−15.
(8) Srivastava, M.; Srivastava, S. K.; Nirala, N. R.; Prakash, R. *Anal. Methods* **2014**, *6*, 817−824.
(9) Zhang, M.; Yuan, R.; Chai, Y.; Wang, C.; Wu, X. *Anal. Biochem.* **2013**, *436*, 69−74.
(10) Yang, J.; Lee, H.; Cho, M.; Nam, J.; Lee, Y. *Sensor. Actuators, B* **2012**, *171−172*, 374−379.
(11) Singh, J.; Srivastava, M.; Kalita, P.; Malhotra, B. D. *Process Biochem.* **2012**, *47*, 2189−2198.
(12) Arya, S. K.; Pandey, P.; Singh, S. P.; Datta, M.; Malhotra, B. D. *Analyst* **2007**, *132*, 1005−9.
(13) Numnuam, A.; Thavarungkul, P.; Kanatharana, P. *Anal. Bioanal. Chem.* **2014**, *406*, 3763−3772.
(14) Zhang, Y.; Wen, G.; Zhou, Y.; Shuang, S.; Dong, C.; Choi, M. M. *Biosens. Bioelectron.* **2007**, *22*, 1791−7.
(15) Rawal, R.; Chawla, S.; Chauhan, N.; Dahiya, T.; Pundir, C. S. *Int. J. Biol. Macromol.* **2012**, *50*, 112−8.
(16) Bhawna; Pundir, C. S. *J. Sci. Ind. Res. India* **2010**, *69*, 695−699.
(17) Pan, L. J.; Yu, G. H.; Zhai, D. Y.; Lee, H. R.; Zhao, W. T.; Liu, N.; Wang, H. L.; Tee, B. C.; Shi, Y.; Cui, Y.; Bao, Z. N. *Proc. Natl. Acad. Sci. U.S.A.* **2012**, *109*, 9287−92.
(18) Zhai, D. Y.; Liu, B.; Shi, Y.; Pan, L. J.; Wang, Y. Q.; Li, W. B.; Zhang, R.; Yu, G. H. *ACS Nano* **2013**, *7*, 3540−6.
(19) Wang, Z.; Ma, Y.; Hao, X.; Huang, W.; Guan, G.; Abudula, A.; Zhang, H. *J. Mater. Chem. A* **2014**, *2*, 15035−15043.
(20) Behera, S.; Raj, C. R. *Biosens. Bioelectron.* **2007**, *23*, 556−561.
(21) Ahmadalinezhad, A.; Chen, A. *Biosens. Bioelectron.* **2011**, *26*, 4508−4513.
(22) Dey, R. S.; Raj, C. R. *J. Phys. Chem. C* **2010**, *114*, 21427−21433.
(23) Wu, C.; Liu, X.; Li, Y.; Du, X.; Wang, X.; Xu, P. *Biosens. Bioelectron.* **2014**, *53*, 26−30.
(24) Dhand, C.; Solanki, P. R.; Datta, M.; Malhotra, B. D. *Electroanal.* **2010**, *22*, 2683−2693.
(25) Li, G.; Liao, J. M.; Hu, G. Q.; Ma, N. Z.; Wu, P. J. *Biosens. Bioelectron.* **2005**, *20*, 2140−2144.
(26) Ali, M. A.; Srivastava, S.; Solanki, P. R.; Reddy, V.; Agrawal, V. V.; Kim, C.; John, R.; Malhotra, B. D. *Sci. Rep.* **2013**, *3*, 2661.
(27) Sun, C. L.; Chang, C. T.; Lee, H. H.; Zhou, J.; Wang, J.; Sham, T. K.; Pong, W. F. *ACS Nano* **2011**, *5*, 7788−7795.
(28) Zhao, Y.; Liu, B. R.; Pan, L. J.; Yu, G. H. *Energy Environ. Sci.* **2013**, *6*, 2856−2870.
(29) Zheng, G. F.; Patolsky, F.; Cui, Y.; Wang, W. U.; Lieber, C. M. *Nat. Biotechnol.* **2005**, *23*, 1294−1301.
(30) Taurino, I.; Magrez, A.; Matteini, F.; Cavallini, A.; Forro, L.; De Micheli, G.; Carrara, S. *Nano Lett.* **2014**, *14*, 3180−3184.
(31) Penner, S.; Stöger-Pollach, M.; Thalinger, R. *Catal. Lett.* **2014**, *144*, 87−96.
(32) Luo, Y. C.; Do, J. S.; Liu, C. C. *Biosens. Bioelectron.* **2006**, *22*, 482−488.
(33) Safavi, A.; Farjami, F. *Biosens. Bioelectron.* **2011**, *26*, 2547−2552.
(34) Lian, Q.; He, Z.; He, Q.; Luo, A.; Yan, K.; Zhang, D.; Lu, X.; Zhou, X. *Anal. Chim. ACTA* **2014**, *823*, 32−39.
(35) Thakur, B.; Sawant, S. N. *ChemPlusChem.* **2013**, *78*, 166−174.
(36) Singh, S.; Solanki, P. R.; Pandey, M. K.; Malhotra, B. D. *Sensor. Actuators, B* **2006**, *115*, 534−541.
(37) Singh, S.; Solanki, P. R.; Pandey, M. K.; Malhotra, B. D. *Anal. Chim. ACTA* **2006**, *568*, 126−32.
(38) Vidal, J. C.; Espuelas, J.; Garcia-Ruiz, E.; Castillo, J. R. *Talanta* **2004**, *64*, 655−664.
(39) Narang, J.; Chauhan, N.; Pundir, C. S. *Int. J. Biol. Macromol.* **2013**, *60*, 45−51.
(40) Minakshi, C.; Pundir, C. S. *Sensor. Actuators, B* **2008**, *133*, 251−255.

DOI: 10.1021/nl504217p
Nano Lett. 2015, 15, 1146−1151